Design and analysis of VCSEL based two-dimension wavelength converter

H. Liu and P. Shum
Network Technology Research Center,Nanyang Technological University
Singapore 639798
liuhairong@pmail.ntu.edu.sg, epshum@ntu.edu.sg

M. S. Kao
Department of Communication Engineering,National Chiao-Tung University
Hsinchu, Taiwan, 30050
mskao@cc.nctu.edu.tw

Abstract: A novel two-dimensional vertical cavity surface emission laser (VCSEL) based wavelength converter is proposed. We developed a two-dimensional transmission line laser model (TLLM) to analyze the proposed wavelength converter. This model takes into account Bragg reflectors by using the modified connecting matrix. Therefore, accurate and efficient modeling of the VCSEL structure is achieved. Extinction ratio of the output signal is investigated by considering input signal power, wavelength, facet reflectivity and cavity diameter.

OCIS codes: (140.5960) Semiconductor lasers; (140.4480) Optical amplifiers

References and links

1. T. Durhuus, B. Mikkesen, C. Joergensen, S. L. Danieselen, and K. E. Stubjkaer, " All-optical wavelength conversion by semiconductor optical amplifiers," J. Lightwave Technol. **14**, 943-954 (1996)
2. S.L. Danielsen, P.B.Hansen, and K.E. Stubjær, "Wavelength conversion in optical packet switching," J. Lightwave Technol. **16**, 2095-2108 (1998)
3. K. Obermann, S. Kindt, D. Breuer, and K. Petermann, " Performance analysis of wavelength converters based on cross-gain modulation in semiconductor-optical amplifiers," J. Lightwave Technol. **16**, 78-85 (1998)
4. K. Nonaka, H. Tsuda, H. Uenohara, H. Iwamura and T. Kurokawa, "Optical nonlinear characteristics of a side-injection light-controlled laser diode with a multiple-quantum-well saturable absorption region," IEEE Photon. Technol. Lett. **5**, 139-141 (1993)
5. K. Nonaka, F. Kobayashi, K. Kishi, T. Tadokoro,Y. Itoh, C. Amano, and T. Kurokawa, "Direct Time Domain Optical Demultiplexing of 10-Gb/s NRZ signals using side-injection light-controlled bistable laser diode," IEEE Photon. Tech. Lett. **10**, 1484-1486 (1998)
6. E. Höfling, R. Werner, F. Schäfer, J.P. Reithmaier and A. Forchel, " Short-cavity edge-emitting lasers with deeply etched distributed Bragg mirrors," Electron. Lett. **35**, 154-155 (1999)
7. K. Iga, "Surface-emitting laser-its birth and generation of new optoelectronics field," IEEE J. Select. Topics Quantum Electron. **6**, 1201-1215 (2000)
8. J. Cheng and N. K.Dutta, *Verical-cavity surface-emitting lasers: technology and applications*, (Gordon and Breach Science Publishers, 2000), Chap 1
9. S.F.Yu, "Dynamic behavior of vertical-cavity surface-emitting lasers," IEEE J. Quantum Electron. **32**, 1168-1179 (1996)
10. S.F.Yu, "An improved Time-Domain Travelling-Wave model for vertical-cavity surface-Emitting lasers," IEEE J. Quantum Electron. **34**, 1938-1948 (1998)
11. A. J. Lowery, " Transmission-line modeling of semiconductor lasers: the transmission-line laser model ", Internaltional Journal of numerical modeling: Electronic Networks, Devices and Fields, **2**, 249-265 (1989)
12. H. Lee, H. Yoon, Y. Kim, and J. Jeong, "Theoretical study of frequency chirping and extinction ration of wavelength-converted optical signals by XGM and XPM using SOA's," IEEE J. Quantum Electron. **35**, 1213-1219 (1999)
13. A.J.Lowery, "Dynamic modeling of distributed-feedback lasers using scattering matrices," Electron. Lett. **25**, 1307-1308 (1989)

#2461 - $15.00 US Received May 07, 2003; Revised July 01, 2003

14. L.V.T. Nguyen, A.J. Lowey, P.C.R. Gurney, and D.Novak, " A time domain model for high speed quantum well lasers including carrier transport effects," IEEE J. Sel. Top. Quantum Electron. **1**, 494-504 (1995)
15. P.J. Annets, M.Asghari and I.H. White, " The effect of carrier transport on the dynamic performance of gain-saturation wavelength conversion on MQW semiconductor optical amplifiers," IEEE J. Sel. Top. Quantum Electron. **3,** 320-329 (1997)

1. Introduction

Semiconductor optical amplifier (SOA) based wavelength converters have the potential to support wavelength switching in WDM optical networks [1,2]. In the wavelength converter an intensity modulated input signal at the wavelength λ_{Signal} (called signal) is used to modulate the carrier density of the SOA. With the modulation of the λ_{Signal}, the (inverted) data can be copied onto another continuous wave on the wavelength λ_{Probe} (called probe). The signal wave and the probe wave can be injected into the SOA either co- or counter-propagating (Fig. 1). However, shortcomings exist in both of these configurations. For the co-propagating injection, an optical filter is needed to suppress the signal wave. For the counter-propagating method, though optical filter is avoided, an additional isolator at the probe input is needed to suppress the strongly amplified input signal. Moreover, in the latter configuration smaller bandwidth as well as an enhanced amplified spontaneous emission (ASE) noise level are suffered [3].

Two dimensional side-injection light-controlled bistable laser diodes (SILC-BLD) have been reported by K. Nonaka [4,5]. These reports revealed that SOA based 2-D devices were quite promising for optical signal processing. In this paper a novel two-dimensional VCSEL based wavelength converter is proposed. In this configuration, the VCSEL acts as the laser source for the probe wave and as the SOA to perform the cross-gain modulation. The probe wave and the signal wave will propagate along orthogonal directions with the advantage of simplifying the structure. We develop a modified transmission line laser model (TLLM) to describe the VCSEL based wavelength converter. The dynamic characteristics of the proposed wavelength converter have been investigated.

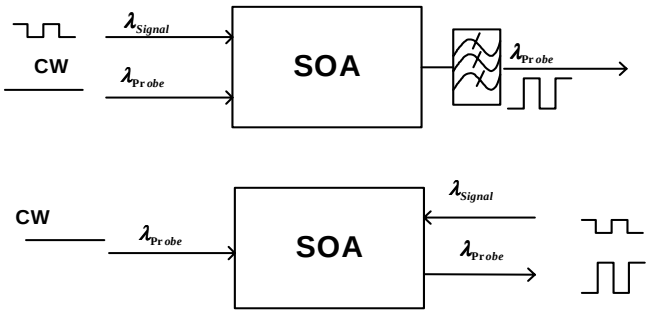

Fig. 1. Co-propagating and counter-propagating wavelength converter

2. VCSEL based two-dimension wavelength converter

To remove the optical filter or the optical isolator from the wavelength converters, the probe wave and the signal wave can be incident on the SOA along orthogonal directions (Fig. 2(a)). Owing to the limitation of the incident wave intensity, the length of the SOA should be very

#2461 - $15.00 US Received May 07, 2003; Revised July 01, 2003

short. However, the cavity as short as $10\,\mu m$ is very difficult to fabricate [6], and it is not easy to get stable operation condition for such short cavity laser. To overcome this difficulty, VCSEL can be employed for the advantage of its short cavity [7,8]. A novel VCSEL based wavelength converter is proposed as shown in Fig. 2(b). Here we adopted the VCSEL structure [9,10] and extended the active region at the horizontal direction. In the configuration, the signal wave will incident at the horizontal direction and the probe wave will output at the vertical direction, thereby a two-dimension wavelength converter is realized. In this structure, the extended active region was used to amplify the input signal wave, which guarantees a strong cross-gain modulation effect. By this means, high extinction ratio of the probe wave can be achieved.

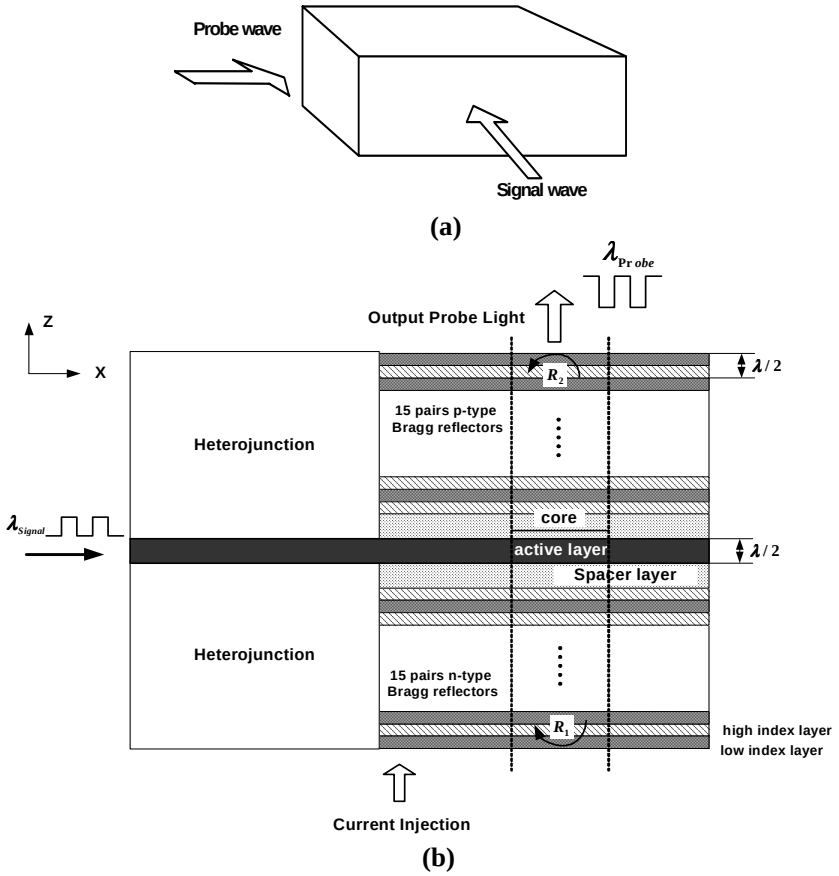

Fig. 2. (a) Schematic of two-dimension wavelength converter. (b) VCSEL based two-dimension wavelength converter

In the proposed configuration, the VCSEL is used both as the laser source for the probe wave and as SOA for performing cross-gain modulation. By employing this structure, two main advantages will be provided. First, additional devices such as optical filter or optical isolator, are not required anymore. Second, additional laser source for the probe wave can be saved because VCSEL works as a laser source as well as an amplifier.

3. Two-dimension transmission line laser model

To analyze the characteristics of the proposed structure, a two-dimension TLLM is required. Details of one-dimension TLLM had been given in Ref. [11]. The schematic of the modified

#2461 - $15.00 US Received May 07, 2003; Revised July 01, 2003

TLLM model for the two-dimension VCSEL based wavelength converter is shown in Fig.3. In the developed model the forward and backward probe waves are named as F_P and B_P, and those of the signal wave are named as F_S and B_S, respectively. We describe the scattering process at time t of these four waves in the active region as:

$$ {}_t[F_P(n,m)]^r = S_p *_t [F_P(n,m)]^i + {}_t[I_{sp}(n,m) Z_p T/2] \quad (1) $$

$$ {}_t[B_P(n,m)]^r = S_p *_t [B_P(n,m)]^i + {}_t[I_{sp}(n,m) Z_p T/2] \quad (2) $$

$$ {}_t[F_S(n,m)]^r = S_S *_t [F_S(n,m)]^i + {}_t[I_{sp}(n,m) Z_p T/2] \quad (3) $$

$$ {}_t[B_S(n,m)]^r = S_S *_t [B_P(n,m)]^i + {}_t[I_{sp}(n,m) Z_p T/2] \quad (4) $$

where i denotes the incident wave, r denotes the reflective wave, S_S is the scattering matrix for the signal wave, S_P is the scattering matrix for the probe wave, I_{sp} is the spontaneous noise current, T is the attenuation factor, n and m are the section numbers in the traveling direction of the probe wave and the signal wave, respectively. Z_p is the cavity wave impedance given as $Z_p = \overline{n_e} 120\pi / n_e$, where $\overline{n_e}$ is the effective group index, n_e is the effective index, Scattering matrices S_S and S_P can be found in [11]. The ASE noise is modeled with noise current I_{sp}, which is represented by three statistically independent Gaussian distributed random processes that satisfy the following correlation [11,12]:

$$ \left\langle I_{sp}(z,x,t) I_{sp}^{*}(z,x,t) \right\rangle = 2\beta L R_{sp} \delta(z-z') \delta(x-x') \delta(t-t') \times hf / Z_p \quad (5) $$

where β is the spontaneous coupling factor, R_{sp} is the spontaneous emission rate which is assumed as bimolecular recombination (BN^2), $\delta(x)$ is the Delta-function, hf is the photon energy and L is the laser cavity length.

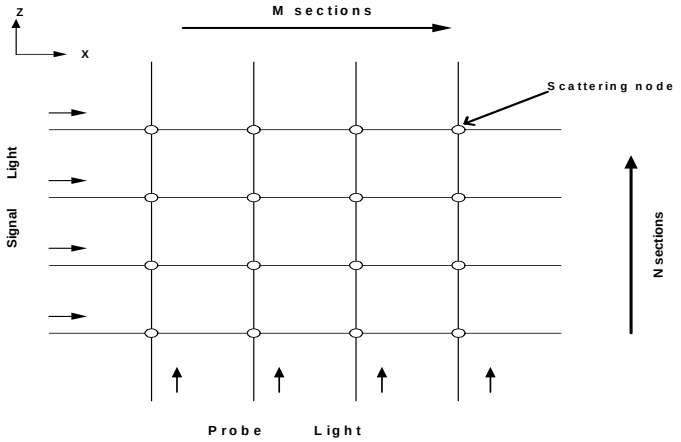

Fig. 3. Schematic of the two-dimension TLLM

#2461 - $15.00 US
Received May 07, 2003; Revised July 01, 2003

The information of the material gain is required in the scattering process. In our model material gain depends on both the carrier density and the wavelength, given as [12]

$$g(N,\lambda_k)=\frac{a_0\ln(N/N_0)-a_1(\lambda_k-\lambda_p)^2+a_2(\lambda_k-\lambda_p)^3}{1+\varepsilon(P_S+P_P)} \tag{6}$$

where a_0 , a_1 ,and a_2 are gain constants, λ_P the gain-peak wavelength, ε the gain compression factor, N the local carrier density, N_0 the transparent carrier density. The gain for the probe wave or the signal wave can be obtained when λ_k is set as λ_{Probe} or λ_{Signal}.

The connecting process which connects two scattering nodes together can be written as [11]:

$$_{t+1}\left[F_P(n+1,m)\right]^i = C_p *_t \left[F_P(n,m)\right]^r \tag{7}$$

$$_{t+1}\left[B_P(n,m)\right]^i = C_p *_t \left[B_P(n+1,m)\right]^r \tag{8}$$

$$_{t+1}\left[F_S(n,m+1)\right]^i = C_S *_t \left[F_S(n,m)\right]^r \tag{9}$$

$$_{t+1}\left[B_S(n,m)\right]^i = C_S *_t \left[B_P(n,m+1)\right]^r \tag{10}$$

where C_P is the connecting matrix for the probe wave and C_S is the connecting matrix for the signal wave. It should be noted that C_P and C_S are identity matrices for those sections where there are no distributed Bragg reflectors (DBR) such that no reflections happen between forward waves and backward waves.

However, out of the cross-gain modulation area, DBR exists in the vertical direction. In these sections C_P is not identity matrix anymore and should be modified to reflect the wave coupling and reflection in DBR. The connecting process in these sections is described as

$$_{t+1}\begin{bmatrix} F_P(n+1,m) \\ B_P(n,m) \end{bmatrix}^i = C_P * _t\begin{bmatrix} F_P(n,m) \\ B_P(n+1,m) \end{bmatrix}^r \tag{11}$$

In the previous model, gratings can be modeled by connecting two adjacent scattering matrices with impedance unmatched transmission lines [13]. However, the coupling coefficient is difficult to calculate and can't well reflect the effects of the DBR in VCSEL. To represent wave changes at the Bragg reflectors, we employ the connecting matrices using effective index method [9]:

$$C_P=\begin{bmatrix} 2\sqrt{n_l n_h}\,/\,(n_l+n_h) & -(n_l-n_h)\,/\,(n_l+n_h) \\ (n_l-n_h)\,/\,(n_l+n_h) & 2\sqrt{n_l n_h}\,/\,(n_l+n_h) \end{bmatrix} \tag{12}$$

which represents the connecting matrix when the wave travel from low-index layer to high-index layer and

#2461 - $15.00 US Received May 07, 2003; Revised July 01, 2003

$$C_P = \begin{bmatrix} 2\sqrt{n_l n_h}\,/\,(n_l + n_h) & -(n_h - n_l)\,/\,(n_l + n_h) \\ (n_h - n_l)\,/\,(n_l + n_h) & 2\sqrt{n_l n_h}\,/\,(n_l + n_h) \end{bmatrix} \tag{13}$$

which describes the wave traveling from the high-index to low-index layer layer. Here n_l is the effective index of the low index layer and n_h is the effective index of the high index layer.

After the scattering and connecting processes, local photon density can be obtained from the local field intensity [11]. Carrier density will be updated with the information of the local photon density. The carrier density will be determined by the photon density of both probe wave and signal wave, given as [14,15]

$$\frac{dN_{MQW}}{dt} = \frac{N_{SCH}}{\tau_r} \cdot \frac{d_{SCH}}{d_{MQW}} - \frac{N_{MQW}}{\tau_e} - \frac{N_{MQW}}{\tau_{rec(MQW)}} - v_g(\Gamma_P g_P P_P + \Gamma_S g_S P_S) \tag{14}$$

$$\frac{dN_{SCH}}{dt} = \frac{J}{e \cdot d_{SCH}} - \frac{N_{SCH}}{\tau_r} + \frac{N_{MQW}}{\tau_e} \cdot \frac{d_{MQW}}{d_{SCH}} - \frac{N_{SCH}}{\tau_{rec(SCH)}} \tag{15}$$

where N_{MQW} is the carrier density in the multiple quantum well active layer, N_{SCH} the carrier density in the separate confinement layer, d_{MQW} and d_{SCH} the thickness of the active layer and the separate confinement layer, respectively; v_g is the group velocity, τ_e the carrier emission constant, τ_{rec} the recombination time and τ_r the carrier diffusion time, e the charge of the electron, J the injection current density, P_S and P_P the photon densities, g_S and g_P the material gains of the signal wave and the probe wave, respectively.

4. Results and discussion

We have analyzed the proposed structure by applying the proposed TLLM. Simulation parameters are given in Table 1. Time domain response has been investigated at the bit rate of 2.5Gbits/s. Figure 4 shows the pulse pattern of probe wave (upper) and signal wave (lower). In the simulation the signal wave is located at the gain-peak and the probe wavelength was at –40nm shift from the gain-peak, i.e., $\lambda_{signal} = 1565nm$ and $\lambda_{probe} = 1525nm$. We observe that the probe signal undergoes overshoot on the rising edge. This can be explained by the fact that the carriers are greatly consumed by the signal wave when it is at high state (‘1’ state), thus the front end of the probe wave experiences overshoot in the gain recovery process when the signal wave at the low state (‘0’ state). The result also reveals that the ‘1’ state power of the signal wave is as high as 25mw to get an extinction ratio of the probe wave larger than 10dB. This is the reason why we have to amplify the signal wave first before cross-gain modulation. In the simulation the input signal powers refer to the power after amplification. Moreover the affect of ASE noise on the probe wave can be seen in Fig. 4. It is shown that ASE noise at low state is smaller than at high state, since gain saturation may reduce the ASE noise at the high input signal power.

#2461 - $15.00 US Received May 07, 2003; Revised July 01, 2003

Table 1. Simulation Parameters

Parameter	Symbol	Value
Gain peak wavelength	λ	1565 nm
Active layer length	d	$0.75\,\mu m$
Radius of core region	r	$1.125\ \mu m$
Facet reflectivity *	R_1	0.974
Facet reflectivity *	R_2	0.55
Attenuation	T	0.998
Wave impedance	Z_p	123.1Ω
Transparency carrier concentration *	N_0	$2.0\times10^{24}\,m^{-3}$
Spontaneous coefficient	β	5×10^{-4}
Bimolecular recombination	B	$1.4\times10^{-16}\,m^3/s$
Material gain constant	a_0	$1.5\times10^{5}\,m^{-1}$
	a_1	$0.074\times10^{20}\,m^{-3}$
	a_2	$3.155\times10^{25}\,m^{-4}$
Nonlinear gain compression factor	ε	$1.3\times10^{-23}\,m^3$
Confinement factor *	Γ	0.158
Effective index of high-index layer of Bragg reflector *	n_h	3.504
Effective index of low-index layer of Bragg reflector *	n_l	2.952

* Parameter are obtained from [7]

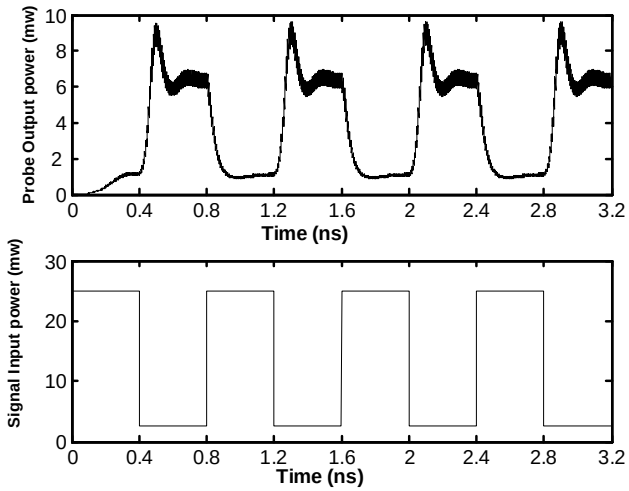

Fig. 4. Pulse pattern of probe wave (upper) and signal wave (lower) at 2.5G (R1=97.4%, R2=55%, $\lambda_{signal}=1565nm$, $\lambda_{probe}=1525nm$, the extinction ratio of input signal=10dB, dotted line represents the steady output power)

#2461 - $15.00 US
Received May 07, 2003; Revised July 01, 2003

To find the optimum signal and probe wavelengths, wavelength-dependent extinction ratio has been studied. Figure 5 shows the contour plot of the output extinction ratio for the signal wavelength and the probe wavelength in the region of 1515~1615nm. Owing to the asymmetric of the gain profile, we observe that down-conversion (λ_{Probe} is shorter than λ_{Signal}) leads to a higher extinction ratio than that of up-conversion (λ_{Probe} is longer than λ_{Signal}). It also shows that high extinction ration can be obtained if λ_{Signal} is around the gain peak.

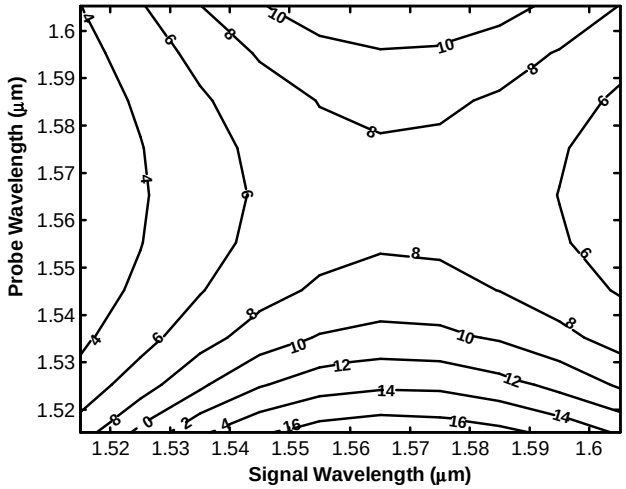

Fig. 5. Contour plot of the extinction ratio with signal wavelength and probe wavelength (R1=97.4%, R2=55%, the extinction ratio of input signal=10dB)

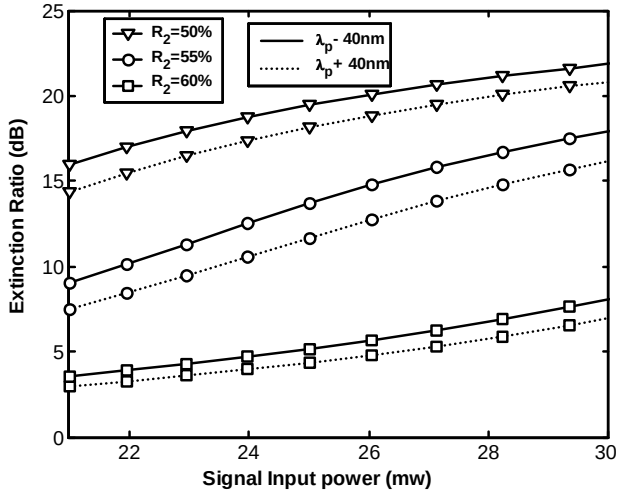

Fig. 6. Extinction ratio of the probe wave as a function of input power of signal wave at different facet reflectivity, with the signal wave located at the peak of the gain curve and probe wave located at 40nm and –40nm shift from the gain peak respect (the solid line $\lambda_{signal} = 1565nm$, $\lambda_{probe} = \lambda_P - 40nm$, i.e., 1525nm, the dotted line $\lambda_{signal} = 1565nm$, $\lambda_{probe} = \lambda_P - 40nm$,i.e.1605nm)

#2461 - $15.00 US Received May 07, 2003; Revised July 01, 2003

We also investigated the effect of different output facet reflectivity on the extinction ratio. As shown in Fig. 6, the extinction ratio of the probe wave increased with the signal power. Moreover, at the same signal power, the extinction ratio decreased as the reflectivity increased. This can be explained as following: when the output facet reflectivity increased, more photons are confined in the cavity leading to enhanced stimulated emission, therefore more carriers are consumed. With decreased carrier density, the gain of the input signal will decrease, which reduces cross-gain modulation effect. In Fig.6 the 40nm down-converted and up-converted cases were simulated. The results showed that down-converted case could obtain higher extinction ratio.

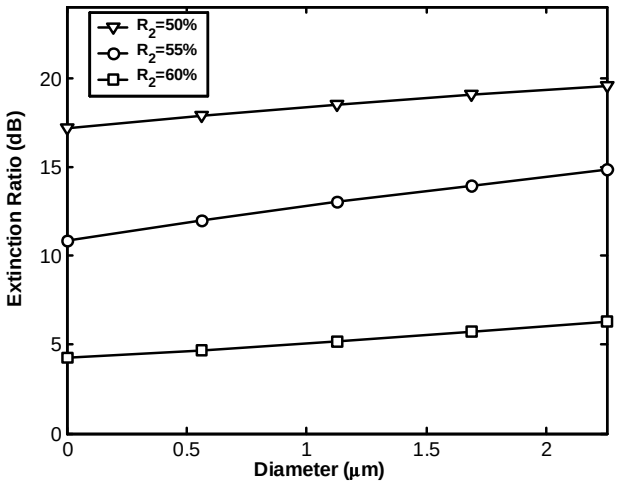

Fig. 7. The evolution of the signal power in the transverse direction of the signal wave at different facet reflectivity ($\lambda_{signal} = 1565nm$, $\lambda_{probe} = 1525nm$, input power=25mW).

The evolution of the signal wave in the transverse direction at different facet reflectivity is shown in Fig. 7. In the simulation the input power is 25mw with 10dB extinction ratio. We observe that the signal power is amplified along the transverse direction. The smaller the reflectivity, the larger the amplifying factor will be obtained. The evolution of the extinction ratio in the transverse direction is shown in Fig. 8. We see that due to the input power is amplified along the transverse direction higher extinction ratio is obtained with the amplified signal.

#2461 - $15.00 US Received May 07, 2003; Revised July 01, 2003

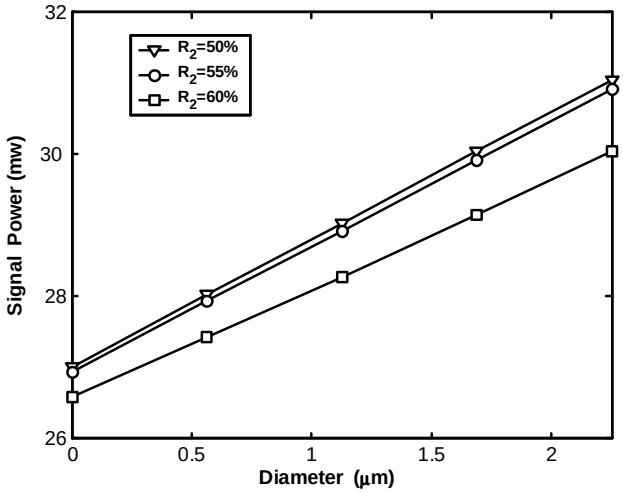

Fig. 8. The evolution of the extinction ratio in the transverse direction of the probe wave at different facet reflectivity. ($\lambda_{signal} = 1565nm$, $\lambda_{probe} = 1525nm$, input power=25mW).

5. Conclusion

We proposed a novel two-dimensional VCSEL based wavelength converter and analyzed it using our developed TLLM. The proposed VCSEL is used both as the laser source for the probe wave and as an SOA for performing cross-gain modulation. The developed TLLM model provides an accurate tool to analyze the dynamic characteristics of the VCSEL based wavelength converter. In our analysis, extinction ratio, facet reflectivity, wavelength location as well as the variation of the field along the VCSEL diameter are taken into account. We show that a wideband wavelength converter can be designed by employing the proposed structure.

Acknowledgements

The authors would like to acknowledge the advice and encouragement coming from H. G. Shiraz. They also thank W. J. Lai for fruitful discussion.

#2461 - $15.00 US Received May 07, 2003; Revised July 01, 2003